applied optics

Spherical aberration-based compensation method for narcissus

Lei Li,[1,2,3] Xing Zhong,[3,4,*] Zheng Qu,[1,2] Guangqing Xia,[5,6] Yuanhang Wang,[1,2,3] and Chaoli Zeng[4,5]

[1]Changchun Institute of Optics, Fine Mechanics and Physics, Chinese Academy of Sciences, Changchun 130033, China
[2]University of Chinese Academy of Sciences, Beijing 100049, China
[3]Chang Guang Satellite Technology Co., Ltd, Changchun 130102, China
[4]Key Laboratory of Advanced Technology for Aerospace Vehicles of Liaoning Province, Dalian University of Technology, Dalian 116024, China
[5]State Key Laboratory of Structural Analysis, Optimization and CAE Software for Industrial Equipment, Dalian University of Technology, Dalian 116024, China
[6]Collaborative Innovation Center of Micro & Nano Satellites of Hebei Province, North China Institute of Aerospace Engineering, Langfang 065000, China
*zhongxing@charmingglobe.com

Received 1 August 2023; revised 31 October 2023; accepted 7 November 2023; posted 8 November 2023; published 22 November 2023

A narcissus-compensation method is proposed based on a mathematical model that connects the spherical aberration and the narcissus-induced temperature difference (NITD). Through non-sequential ray tracing analysis in ZEMAX, we simulate a compact, five-lens, long-wave infrared (LWIR) optical system with NITD as low as 0.7 mK.

https://doi.org/10.1364/AO.502095

1. INTRODUCTION

For cooled infrared imaging systems, narcissus is generated by the temperature difference between a cold detector and a warm environment, and the radiation from the detector is reflected back to the detector from the surface of the lens in the optical system. Narcissus causes the radiation emitted from the detector to overlap with the radiation from the scene incident on the detector, appearing as a black shadow at the center of the raw image, reducing the quality of the image or obscuring important targets in the field of view; hence the need for narcissus suppression [1–4]. There are currently two main methods to suppress narcissus. The first approach is to design the optical system to minimize the narcissus reaching the detector. The second approach is to treat narcissus as a form of low-frequency image noise and eliminate it from the raw image through image processing techniques [5,6].

In the process of narcissus optimization, the magnitude of the narcissus is now commonly measured by the paraxial parameter yni, which indicates the degree of defocusing of the reflected light from the center of the field of view and is limited to control narcissus in the optimization of the optical system. This method allows for a quick and easy optimization of narcissus, but not an accurate representation [7]. After the optimization of narcissus, the exact representation of narcissus is divided into two main methods. In the sequential ray tracing method, the light travels sequentially from one surface to the next, and only polished lens surfaces can be modeled, while rough mechanical surfaces cannot be modeled. Therefore, this allows for a relatively fast and accurate representation of narcissus. In the non-sequential ray tracing method, the rays are not required to follow any particular sequence, but they are emitted from the detector and are refracted or reflected according to the properties of the optical surfaces in their path until they return to the detector, and the number of rays reflected back to the detector is counted, and then the narcissus-induced temperature difference (NITD) is calculated. This method provides a more accurate representation of narcissus but is very time-consuming and cannot be implemented in the system optimization process [8–12]. The narcissus optimization method can only reduce the magnitude of the narcissus under the premise of meeting the imaging quality requirements, and the optimized narcissus is still large. In the process of narcissus elimination, variations in image quality caused by narcissus can be seen as a result of the non-uniformity of the detector response. Therefore, narcissus can theoretically be eliminated by non-uniformity correction [13,14]. Current low-frequency non-uniform image noise calibration algorithms mainly include iterative optimization algorithms for low-frequency fixed-pattern noise, algorithms based on deep learning, and noise estimation algorithms for fixed patterns [15–17], all of which are used to eliminate narcissus through image processing, and the use of optical system optimization to eliminate non-uniformity has not been investigated.

In this paper, a mathematical model of the relationship between spherical aberration and yni is first established from the spherical aberration model of the optical system. After that, the definition of spherical aberration shows that the spherical

aberration varies quadratically with the incident height, so the relationship between the spherical aberration and the NITD is obtained. Optimization of the spherical aberration can obtain a system with NITD close to zero and achieve non-uniformity correction, and this method is defined as the narcissus compensation method. Finally, this paper chooses the non-sequential ray tracing method to represent the narcissus, and the macro analysis in ZEMAX can accurately calculate the NITD of each surface of the optical system. The effectiveness and superiority of the narcissus suppression method are demonstrated by analyzing the narcissus.

2. THEORY OF NARCISSUS COMPENSATION

A. Relationship Between Spherical Aberration and *yni*

The narcissus is generated by the detector imaging itself through the reflection of the lens. The height of the light emitted from the center of the detector, reflected by the lens and imaged on the detector y'_r, can be expressed as

$$y'_r = -4yni f\#, \tag{1}$$

where y is the height of the light from the edge of the central field of view incident on the reflective surface, n is the refractive index at the reflective surface, i is the angle of reflection, and $f\#$ is the ratio of the focal length to the aperture of the optical system. For a defined system, $f\#$ is a fixed value, so the magnitude of the narcissus is measured by yni. For an infrared imaging system, the mathematical model for the spherical aberration of the front surface of the lens SPHA_1 can be expressed as [18]

$$\mathrm{SPHA}_1 = \left(\frac{y}{n}\right)(u_1 - yC_1)^2(u'_1 - nu_1). \tag{2}$$

The mathematical model for the spherical aberration on the rear surface of the lens SPHA_2 can be expressed as [18]

$$\mathrm{SPHA}_2 = -\left(\frac{y}{n}\right)(u'_2 - yC_2)^2(u_2 - nu'_2), \tag{3}$$

where u_1 is the angle of incidence on the front surface of the lens, u'_1 is the angle of refraction on the front surface of the lens, C_1 is the curvature of the front surface of the lens, u_2 is the angle of incidence on the rear surface of the lens, u'_2 is the angle of refraction on the rear surface of the lens, and C_2 is the curvature of the rear surface of the lens, and the spherical aberration of the lens is modified to obtain the relationship between the spherical aberration of the front surface of the lens and yni:

$$\begin{aligned}
\mathrm{SPHA}_1 &= \left(\frac{y}{n}\right)(u_1 - yC_1)^2(u'_1 - nu_1)\\
&= \left(\frac{y}{n}\right) i_1^2\left[u_1 + i_1 - i'_1 - n\left(yC_1 - i_1\right)\right]\\
&= yni'^2_1\left[(1-n)yC_1 + (n^2-1)i'_1\right]\\
&= (1-n)\frac{(yni'_1)^2 C_1}{n} + (n^2-1)\frac{(yni'_1)^3}{n^2y^2}\\
&= \frac{(n-1)}{ny}(yni'_1)^2\left(\frac{yni'_1}{ny} - u_1\right).
\end{aligned} \tag{4}$$

Similarly, the relationship between the spherical aberration of the rear surface of the lens and yni is

$$\begin{aligned}
\mathrm{SPHA}_2 &= -\left(\frac{y}{n}\right)\left(u'_2 - yC_2\right)^2(u_2 - nu'_2)\\
&= -\left(\frac{y}{n}\right) i'^2_2\left[u'_2 + i'_2 - i_2 - n\left(yC_2 - i'_2\right)\right]\\
&= -\left(\frac{y}{n}\right) i'^2_2\left[(1-n)yC_2 + \left(n - \frac{1}{n}\right) i'_2\right]\\
&= (n-1)\frac{(yni'_2)^2 C_2}{n} + (1-n^2)\frac{(yni'_2)^3}{n^2y^2}\\
&= \frac{(1-n)}{ny}(yni'_2)^2\left(\frac{yni'_2}{ny} - u_2\right).
\end{aligned} \tag{5}$$

From the above model, we can see that $n-1$, $(yni)^2$, and ny are positive, and u_1 and u_2 are constants, so the magnitude of the spherical aberration of the front and rear surfaces of the lens is proportional to the magnitude of yni, from which the narcissus is linked to the spherical aberration of the optical system.

B. Relationship Between Spherical Aberration and Narcissus

After that, it is known from the definition of spherical aberration that on-axis spherical aberration is the deviation of the intersection of light rays of different incident heights with the optical axis relative to the near-axis image point, i.e., $\delta L'$. The on-axis spherical aberration is illustrated in Fig. 1.

Assuming that the optical system consists of k surfaces, the on-axis spherical aberration can be expressed as

$$\delta L' = -\frac{1}{2n'_k u'^2_k}\sum_1^k S_I, \tag{6}$$

where n'_k is the refractive index of the k th surface, u'_k is the angle of emergence of the kth surface, S_I is the spherical aberration of the optical system, and the total spherical aberration of the optical system can be expressed as

$$\begin{aligned}
\sum_1^k S_I &= \sum_1^k hni(i-i')(i'-u)\\
&= \sum_1^k hn\frac{l-r}{r}u(i'u' - iu)\\
&= \sum_1^k h^2 n\left(\frac{1}{r} - \frac{1}{l}\right) ni\left(\frac{u'}{n'} - \frac{u}{n}\right)\\
&= \sum_1^k h^3 Q^2 h\left(\frac{1}{n'l'} - \frac{1}{nl}\right)\\
&= \sum_1^k h^4 Q^2 \Delta\frac{1}{nl}.
\end{aligned} \tag{7}$$

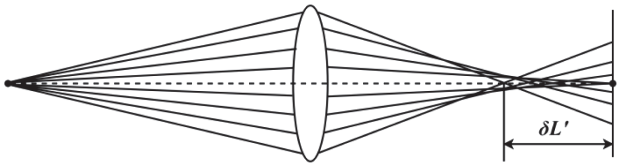

Fig. 1. Schematic diagram of the on-axis spherical aberration.

Therefore, the on-axis spherical aberration can be modified as

$$\delta L' = -\frac{1}{2n'_k l'^2_k}\sum_1^k h^2 Q^2 \Delta\frac{1}{nl}, \tag{8}$$

where h is the incident height, Q is the Abbe invariant. From the above model, it can be seen that n'_k, l'_k, Q, and $\Delta\frac{1}{nl}$ do not vary with the incident height, and the on-axis spherical aberration will vary with the incident height quadratic with the increase of the incident height. Therefore, there is a radiometric difference between the center and the edge of the image plane, and the spherical aberration can be reasonably distributed to compensate for the narcissus. After that, the non-sequential ray tracing method is chosen to accurately represent the narcissus, and the macro analysis in ZEMAX can accurately calculate NITD for each surface of the optical system. The narcissus-induced temperature difference NITD is

$$\mathrm{NITD}_{ij} = \frac{\int_{\lambda_1}^{\lambda_2}\{N(\lambda, T_H) - N(\lambda, T_D)\} R_d(\lambda) t_j(\lambda)^2 R_j(\lambda)\mathrm{d}\lambda}{\int_{\lambda_1}^{\lambda_2}\frac{\partial N(\lambda, T_{MS})}{\partial T} A(\lambda) R_d(\lambda) t_0(\lambda)\mathrm{d}\lambda}\sigma_{ij}, \tag{9}$$

where λ_1, λ_2 is the operating band of the system, T_H is the temperature inside the lens barrel, T_D is the detector temperature, N is the blackbody radiation intensity, t_0 is the spectral transmittance of the whole system, t_j is the average transmittance from the lens surface j to the detector, R_d is the detector spectral response, R_j is the reflectance of the lens surface j, and σ_{ij} is the narcissus of the lens surface j.

The narcissus is generated by the radiation from the detector reflecting back to the detector through the optical system, and the on-axis spherical aberration model after reflection can be expressed as

$$\delta L' = \frac{1}{2n'_k u'^2_k}\sum_1^k S_I. \tag{10}$$

From the above model, it can be seen that n'_k and u'^2_k are positive. Therefore, when the optical system $\sum_1^k S_I < 0$, the center of the image plane receives more radiation than the edges of the image plane at this time, and the corresponding NITD > 0; when the optical system $\sum_1^k S_I > 0$, the center of the image plane receives less radiation than the edges of the image plane at this time, and the corresponding NITD < 0. It can be seen that the positive and negative of the spherical aberration determines the positive and negative of the NITD, and the optimization of the spherical aberration can obtain a system where NITD is close to zero to achieve the non-uniformity correction, and the macro analysis in the narcissus compensation process can accurately obtain the NITD for each surface. The most important aspect of narcissus compensation is to ensure that the optical system can produce both positive and negative NITD. The flow chart of the narcissus compensation method is illustrated in Fig. 2.

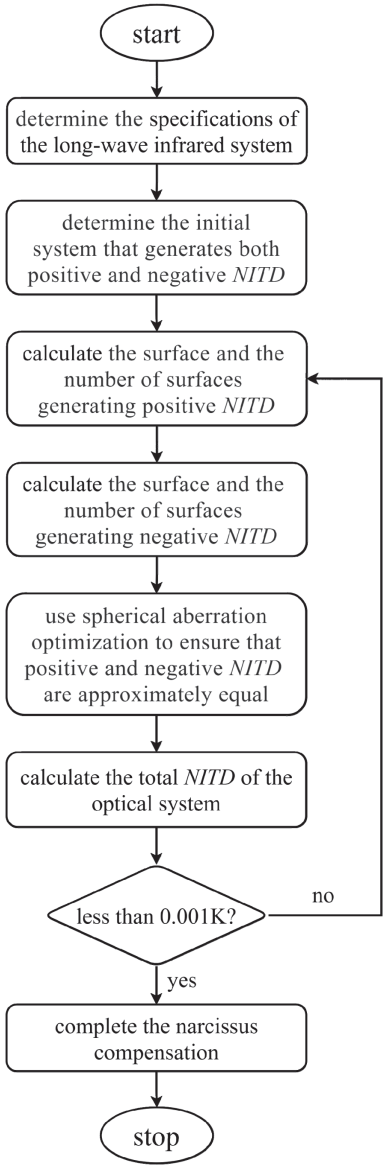

Fig. 2. Flow chart of the narcissus compensation method.

3. NARCISSUS OPTIMIZATION METHOD

A. Specifications and Optical System Design

LWIR cameras have good environmental adaptability, good penetration, and can detect targets that are difficult to be detected by visible light systems, so in this paper we chose to design a LWIR optical system with a large field of view and large relative aperture. The optical specifications are given in Table 1.

The optical system is designed based on the optical specifications, and the optical design parameters are given in Table 2. The optical layout is illustrated in Fig. 3(a), where it can be seen that the optical system consists of five lenses with a compact design, and the total length of the system is less than 60 mm. To ensure

Table 1. Specifications of the LWIR System

Parameter	Value
Focal Length (mm)	24
F-number	1.2
Full-field of View (°)	30 × 30
Spectral Bandwidth (μm)	7.5–13.5
Pixel Size of the Detector (μm)	25
MTF (20 lp · mm^{-1})	> 0.55

Table 2. Lens Data of the LWIR System

Surface	Type	Radius	Thickness	Material
OBJ	Standard	–	∞	
1	Standard	23.802	6	Germanium
2	Aspherical	20.488	8.8	
3	Standard	−22.276	5	IRG201
4	Standard	−116.397	0.5	
5	Standard	38.688	5	IRG206
6	Standard	70.906	0.5	
7	Standard	57.719	5	ZincSulfide
8	Standard	44.209	0.5	
9	Aspherical	35.546	5	IRG206
10	Standard	−76.682	1	
11	Standard	∞	1	Germanium
12	Standard	∞	2	
STO	Standard	∞	15	
IMA	Standard	–	0	

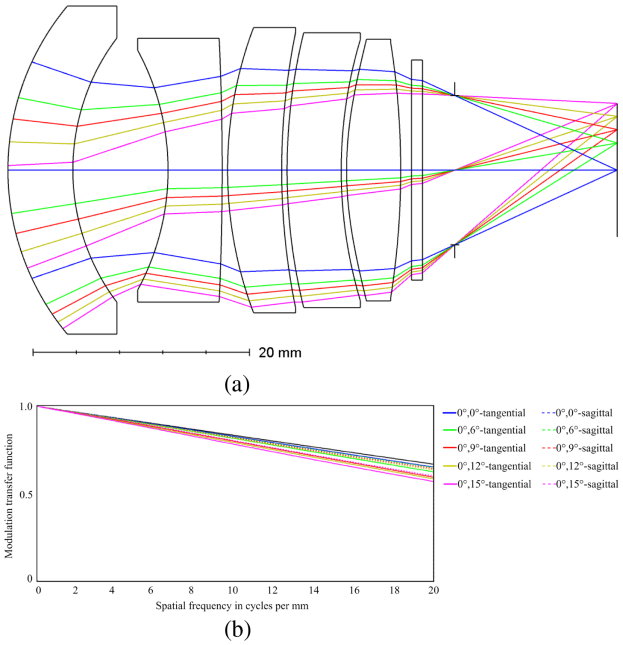

Fig. 3. LWIR system and the image quality evaluation. (a) System layout diagram; (b) modulation transfer function.

that the imaging quality meets the requirements, two aspherical surfaces are introduced in the design, and the MTF is illustrated in Fig. 3(b).

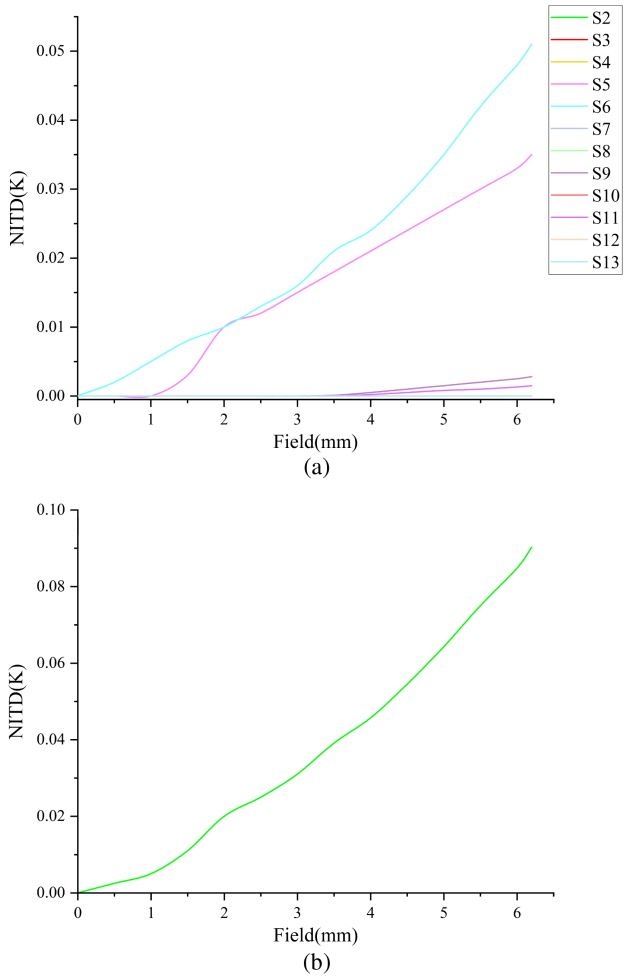

Fig. 4. Narcissus analysis results after the narcissus optimization. (a) NITD for each surface of the system; (b) the total NITD of the system.

B. Narcissus Optimization and Analysis

The magnitude of the narcissus of the optical system is measured by the *yni*. Optimization of narcissus for surfaces with smaller *yni* was carried out to minimize the narcissus while meeting imaging quality requirements. First, the optical system is flipped; the detector is in the object plane and the diaphragm is in surface 1. After that, the lens transmittance is set to 0.99, the detector temperature is set to 77 K, and the temperature of the mechanical structure and the ambient is set to 300 K. Finally, ZEMAX macros are used to analyze NITD. The narcissus analysis results are illustrated in Fig. 4.

From Fig. 4(a), we can see that the total narcissus of the system is composed of the narcissus of several surfaces, where the NITD of surface 6 is 0.051 K, the NITD of surface 7 is 0.035 K, the NITD of surface 9 is 0.0028 K, and the NITD of surface 11 is 0.0015 K. The narcissus of the system is mainly generated by surfaces 6 and 7. From Fig. 4(b), we can see that the total NITD of the system is 0.0903 K, and the narcissus after the narcissus optimization is still large.

4. NARCISSUS COMPENSATION METHOD

A. Initial System Design and Narcissus Analysis

The initial system is designed based on the same specifications, and then the design parameters are calculated. First, the optical system is flipped, the surface of the optical system is set as a reflective surface, and the total spherical aberration of the light emitted from the detector reflected back to the detector after passing through the various surfaces is calculated. After that, the $^{i}/_{\bar{i}}$ of each surface of the optical system is calculated, and the SPHA as well as the $^{i}/_{\bar{i}}$ of the initial system are given in Table 3. The flip layout of the initial system is illustrated in Fig. 5.

The optimization of the narcissus was completed in the previous section, and at this time the total NITD of the optical system is 0.0903 K. Continuing to optimize the narcissus of the optical system will lead to a reduction in the imaging quality. To further suppress the narcissus, this section proposes a spherical aberration-based compensation method for narcissus. The narcissus analysis results of the initial system are illustrated in Fig. 6.

From the theory of narcissus compensation, it can be seen that the positive and negative of the spherical aberration determine the positive and negative of the NITD. As long as the total spherical aberration reflected back to the detector is greater than zero, it is guaranteed that the surface produces a negative NITD. The $^{i}/_{\bar{i}}$ indicates the variation of the narcissus across the detector; the larger the $^{i}/_{\bar{i}}$, the smaller the variation of the narcissus across the detector. As can be seen from Fig. 6, only surface 12 produces a negative NITD. Therefore, a negative NITD can only be generated when the total spherical aberration is greater than zero and the value of $^{i}/_{\bar{i}}$ is sufficiently large.

Table 3. Initial System Design Parameters

Surface	SPHA	$^{i}/_{\bar{i}}$
2	0	1.007255
3	−0.014119	1.006897
4	−0.350688	1.163359
5	−4.170552	0.985266
6	−2.461832	0.578354
7	1.505474	0.586450
8	1.655512	0.577262
9	−2.158699	0.691477
10	4.392740	0.579832
11	5.531589	0.587648
12	1.294981	65.654428
13	0.518746	7.256894

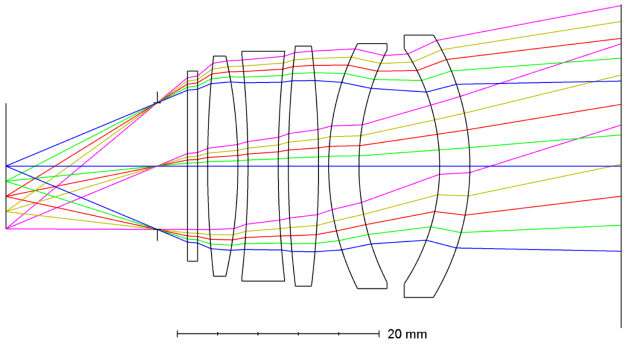

Fig. 5. Flip layout of the initial system.

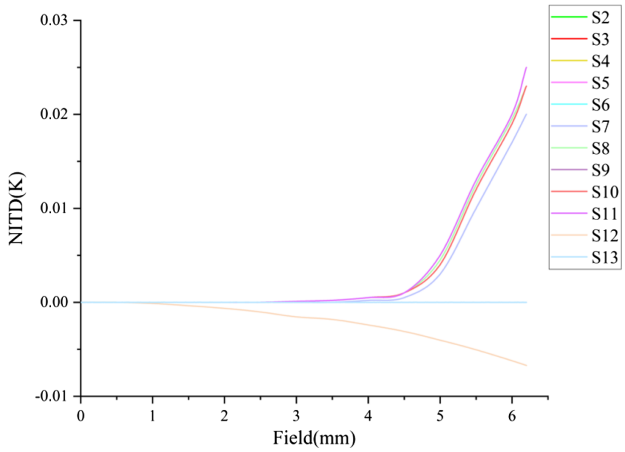

Fig. 6. Narcissus analysis results of the initial system.

Table 4. Lens Data of the Final Optical System

Surface	Type	Radius	Thickness	Material
OBJ	Standard	–	∞	
1	Standard	25.994	6	Germanium
2	Aspherical	21.842	9.3	
3	Standard	−18.847	5.8	ZincSulfide
4	Standard	−26.598	1.8	
5	Standard	35.402	5.1	ZincSulfide
6	Standard	−594.565	0.7	
7	Standard	−248.527	4	ZincSulfide
8	Standard	29.922	1.2	
9	Aspherical	37.102	5	IRG206
10	Standard	−115.205	1	
11	Standard	∞	1	Germanium
12	Standard	∞	2	
STO	Standard	∞	15	
IMA	Standard	–	0	

B. Optical System Design and Narcissus Compensation

After the initial system design, the optical system is optimized to meet specifications and provide good image quality. The optical design parameters are given in Table 4. The optical layout is illustrated in Fig. 7(a), where it can be seen that the design is also compact and the total length of the system is less than 60 mm. The imaging quality meets the requirements, and the MTF is illustrated in Fig. 7(b).

The optimization of the narcissus can only reduce the magnitude of the narcissus, and this optimization has an impact on image quality. In this paper, we propose the narcissus compensation method, which does not need to reduce the NITD for each surface of the optical system but only needs to ensure that the positive and negative NITD of the optical system are approximately equal in magnitude so that the total NITD of the optical system is close to zero. Finally, the same macro analysis in ZEMAX is used to analyze the magnitude of the NITD. The narcissus analysis results after narcissus compensation are illustrated in Fig. 8.

To achieve narcissus compensation, the optical system is ensured to be able to produce both positive and negative NITD as can be seen from Fig. 8(a): surface 5 to surface 11 produces

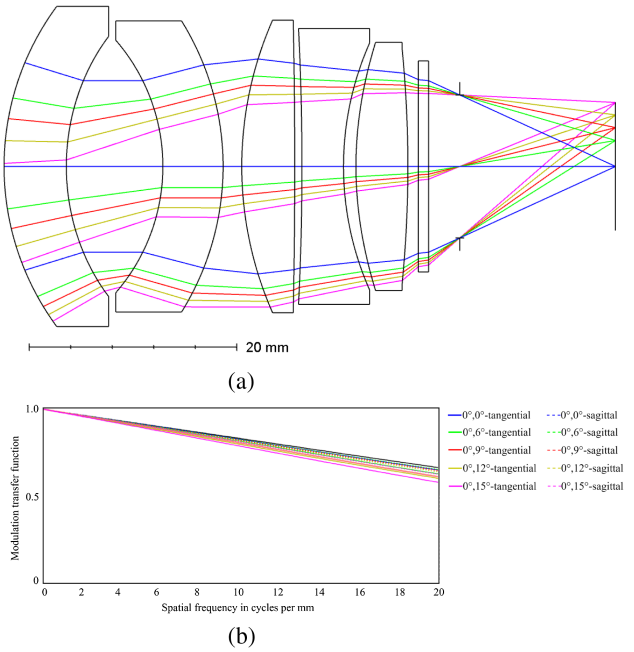

Fig. 7. Final optical system and the image quality evaluation. (a) System layout diagram; (b) modulation transfer function.

positive NITD, and surfaces 12 and 13 produce negative NITD. It can be known that the number of surfaces producing positive NITD is more, so in the process of optical system optimization, the total amount of the negative NITD is first changed to roughly match the total amount of the positive NITD, and then the surfaces producing positive NITD are carefully optimized to match the total amount of negative NITD. This process uses spherical aberration optimization to change the NITD. The narcissus compensation analysis results are illustrated in Fig. 8(b), where the total NITD generated by all surfaces of the optical system is less than 0.7 mK. Compared to the narcissus optimization method, the narcissus compensation method has less impact on image quality because the narcissus compensation process does not need to limit the narcissus for each surface of the optical system too much. The residual narcissus fluctuates with increasing the field of view, and the fluctuations are caused by the compensation errors.

5. CONCLUSION

This paper investigates methods of narcissus suppression and proposes a spherical aberration-based compensation method for narcissus. A mathematical model of the relationship between spherical aberration and yni is first established from the spherical aberration model of the optical system. After that, the definition of spherical aberration shows that the spherical aberration varies quadratically with the incident height, so the relationship between the spherical aberration and the NITD is obtained, and optimization of the spherical aberration can obtain a system with NITD close to zero and achieve non-uniformity correction. Finally, the total NITD is reduced to 0.7 mK after narcissus compensation, which shows that the spherical aberration-based compensation method can effectively suppress narcissus.

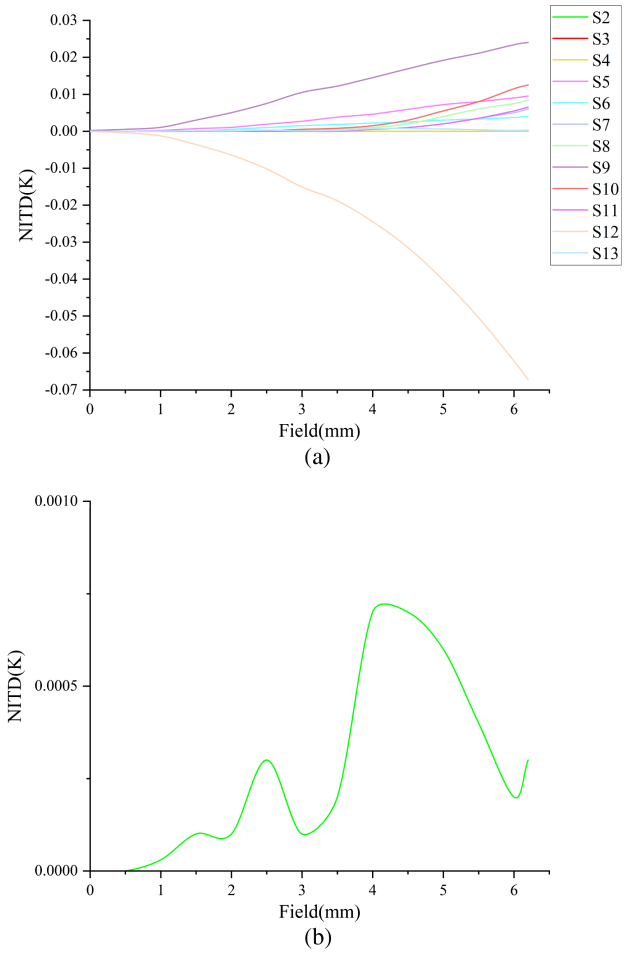

Fig. 8. Narcissus analysis results after the narcissus compensation. (a) NITD for each surface of the system; (b) the total NITD of the system.

Funding. Fundamental Research Funds for the Central Universities (DUT22QN232); National Key Research and Development Program of China (2019YFE0127000, 2020YFC2201100, 2021YFE0116000); National Natural Science Foundation of China (12102082, 12175032, 12211530449, 12275044).

Acknowledgment. This study was co-supported by National Natural Science Foundation of China, National Key R&D Program of China, National Key Research and Development Program of China, the Fundamental Research Funds for the Central Universities of China.

Disclosures. The authors declare no conflicts of interest.

Data availability. Data underlying the results presented in this paper are not publicly available at this time but may be obtained from the authors upon reasonable request.

REFERENCES

1. T. Liu, Q. Cui, C. Xue, and L. Yang, "Calculation and evaluation of narcissus for diffractive surfaces in infrared systems," Appl. Opt. **50**, 2484–2492 (2011).
2. N. Horny, "FPA camera standardisation," Infrared Phys. Technol. **44**, 109–119 (2003).
3. F. He, J. Cui, S. Feng, and X. Zhang, "Narcissus analysis for cooled staring IR system," Proc. SPIE **6722**, 67224N (2007).
4. T. Liu, Q. Cui, L. Yang, C. Xue, and J. Sun, "Evaluation of narcissus for multilayer diffractive optical elements in IR systems," Appl. Opt. **50**, 6146–6152 (2011).

5. S. H. Aslan and S. K. Yerli, "Thin lens narcissus model in infrared lens design with cooled detectors," Appl. Opt. **61**, 728–736 (2022).
6. B. Zhang, Y. F. Hong, and G. H. Shi, "Application of non-uniformity correction to stray radiation suppression of infrared optical system," Opt. Precis. Eng. **12**, 2422–2428 (2008).
7. J. W. Howarda and I. R. Abel, "Narcissus: Reflections on retroreflections in thermal imaging systems," Appl. Opt. **21**, 3393–3397 (1982).
8. K. Lu and S. J. Dobson, "Accurate calculation of Narcissus signatures by using finite ray tracing," Appl. Opt. **36**, 6393–6398 (1997).
9. Y. Liu, X. An, and Q. Wang, "Accurate and fast stray radiation calculation based on improved backward ray tracing," Appl. Opt. **52**, B1–B9 (2013).
10. M. N. Akram, "Simulation and control of narcissus phenomenon using nonsequential ray tracing. I. Staring camera in 3-5 μm waveband," Appl. Opt. **49**, 964–975 (2010).
11. A. V. Pravdivtseva and M. N. Akram, "Simulation and assessment of stray light effects in infrared cameras using non-sequential ray tracing," Infrared Phys. Technol. **60**, 306–311 (2013).
12. Y. Liu, X. Zhong, N. Zhong, C. Zheng, and L. Wen, "Accurate and fast narcissus calculation based on sequential ray trace," Appl. Opt. **52**, 7899–7903 (2013).
13. C. Shia and J. Hao, "A real-time narcissus correction algorithm based on Gaussian mixture models," Infrared Phys. Technol. **117**, 103855 (2021).
14. P. M. McCulloch, C. Olson, and T. D. Goodman, "Eliminating Dewar Narcissus artifacts induced by moving optics in infrared staring focal plane sensors," Proc. SPIE **8486**, 848606 (2012).
15. L. Liu, L. Yan, H. Zhao, X. Dai, and T. Zhang, "Correction of aeroheating-induced intensity nonuniformity in infrared images," Infrared Phys. Technol. **76**, 235–241 (2016).
16. Z. He, Y. Cao, Y. Dong, J. Yang, Y. Cao, and C. L. Tisse, "Single-image-based nonuniformity correction of uncooled long-wave infrared detectors: A deep-learning approach," Appl. Opt. **57**, D155–D164 (2018).
17. C. Liu, X. Sui, Y. Liu, X. Kuang, G. Gu, and Q. Chen, "FPN estimation based nonuniformity correction for infrared imaging system," Infrared Phys. Technol. **96**, 22–29 (2019).
18. J. Sasián, *Introduction to Lens Design* (Cambridge University, 2019).